Inorganic Chemistry

Communication

pubs.acs.org/IC

Miscibility Gap in the U−Nd−O Phase Diagram: a New Approach of Nuclear Oxides in the Environment?

L. Desgranges,*[,†] Y. Pontillon,[†] P. Matheron,[†] M. Marcet,[†] P. Simon,[‡] G. Guimbretière,[‡] and F. Porcher[§]

[†]CEA/DEN/DEC, Bat. 352 Cadarache, 13108 Saint Paul lez Durance, France

[‡]CNRS UPR 3079, CEMHTI, 45071 Orléans Cedex 2, France

[§]CEA/DSM IRAMIS, Centre de Saclay, 91191 Gif sur Yvette, France

Supporting Information

ABSTRACT: To some extent, rare-earth-doped UO_2 is representative of an irradiated nuclear fuel. The two phases we observed previously in neodymium-doped UO_2 are now interpreted as the existence of a miscibility gap in the U−Nd−O phase diagram using new results obtained with Raman spectroscopy. Extrapolating the miscibility gap in the U−Nd−O phase diagram to irradiated UO_2 opens the path to a new understanding of nuclear oxides in the environment.

Predicting the fate of uranium oxides in the environment, whatever their origin, mining, nuclear fuel, or waste, in accidental conditions such as Fukushima earthquake[1] or not, requires precise thermodynamic data. The ability of uraninite to immobilize lanthanide elements over billions of years, which was demonstrated by analysis of the Oklo natural reactor,[2,3] is usually attributed to the existence of a $(U,R)O_{2\pm x}$ phase, where R is a rare-earth element, existing over a large range of R content and oxygen stoichiometry.[4,5] However, most of the data available in the literature describe the behavior of the $(U,R)O_{2\pm x}$ phase at high temperature,[6] and no room temperature phase diagram is available, although these data are obviously mandatory for determination of the uranium oxide impact on the environment. In the present Communication, we give arguments to consider the existence of a miscibility gap in the U−Nd−O phase diagram at room temperature. This result could be extrapolated to many other trivalent doping elements in UO_2 and could lead to a renewed description of the nuclear fuel and its impact on the environment.

In a previous study, we showed by X-ray diffraction the existence of two crystalline phases in several $(U,Nd)O_{2\pm x}$ samples prepared in thermodynamic equilibrium conditions by conventional powder sintering at 1400 °C for 72 h under a 5% Ar/H_2 atmosphere.[7] In this study, these samples were analyzed with Raman spectrometry (633 nm laser excitation line) and neutron diffraction (λ = 1.2251 Å). The new results we obtained give us new arguments for considering the coexisting phases in $(U,Nd)O_{2\pm x}$ samples as proof of a miscibility gap in the U−Nd−O phase diagram.

The existence of these two distinct phases is clearly evidenced by optical microscopy on a cross section of the $(U_{.923},Nd_{.077})O_2$ sample (Figure 1) as white and gray areas (dark areas correspond to the porosity). These phases were characterized by Raman spectroscopy using a focused laser beam with micrometer size. A mapping of Raman spectra measured in a square area on the $(U_{.923},Nd_{.077})O_2$ sample was recorded. Principal component analysis (PCA) was used to extract the main characteristic spectral features corresponding to these two species. The first principal component (PC1) is related to the porosity and will not be discussed here. The two other main principal components (PCs) are associated with the two phases evidenced by optical contrast: PC2 to the white phase and PC3 to the gray phase (Figure 1). PC2 exhibits one peak at 445 cm^{-1} that corresponds to the only active Raman mode in UO_2.[8] PC3 exhibits a UO_2 peak at 445 cm^{-1} and also a broad band that can be decomposed into two peaks: the one at 570 cm^{-1} is attributed to the LO counterpart of the only polar IR-active mode; this Raman component has a resonant character;[9] the other one at 530 cm^{-1} is not reported in the literature (Supporting Information).

The existence of two phases was also evidenced by X-ray and neutron diffraction. These diffraction patterns exhibit two different crystalline phases having a fluorite crystalline structure, the same as UO_2, whose cell parameters were measured[7] (Figure 2). The cell parameter of the first phase has a linear dependence with the Nd content and tends to the UO_2 cell parameter [5.472 (2) Å] for low Nd concentration. It is the only phase detected by diffraction methods on samples with 0.027 and 0.053 M Nd concentration (Figure 2). Therefore, it corresponds to the gray phase observed in Figure 1 because these samples exhibit a gray phase in the Raman spectrum. The cell parameter of the second phase, consequently the white phase, is lower, 5.453(2) Å, with no obvious dependence on the Nd concentration. Although having a similar cell parameter, it is not an oxidized U_4O_9-type phase because superlattice lines, characteristic of U_4O_9,[10] were not observed on the neutron diffraction patterns.

Ohmichi et al. considered two types of $(U,R)O_{2\pm x}$ samples as a function of their O/M ratio (M = U + R) to quantify their changes in the cell parameter.[11] However, they consider continuous variation of the O and Nd contents to interpret their results. The coexistence of two phases with different cell parameters was already observed on $Eu_yU_{1-y}O_{2\pm x}$ samples and was interpreted as metastable phases generated by an inappropriate quenching.[12] This interpretation is not valid in

Received: May 25, 2012
Published: August 20, 2012

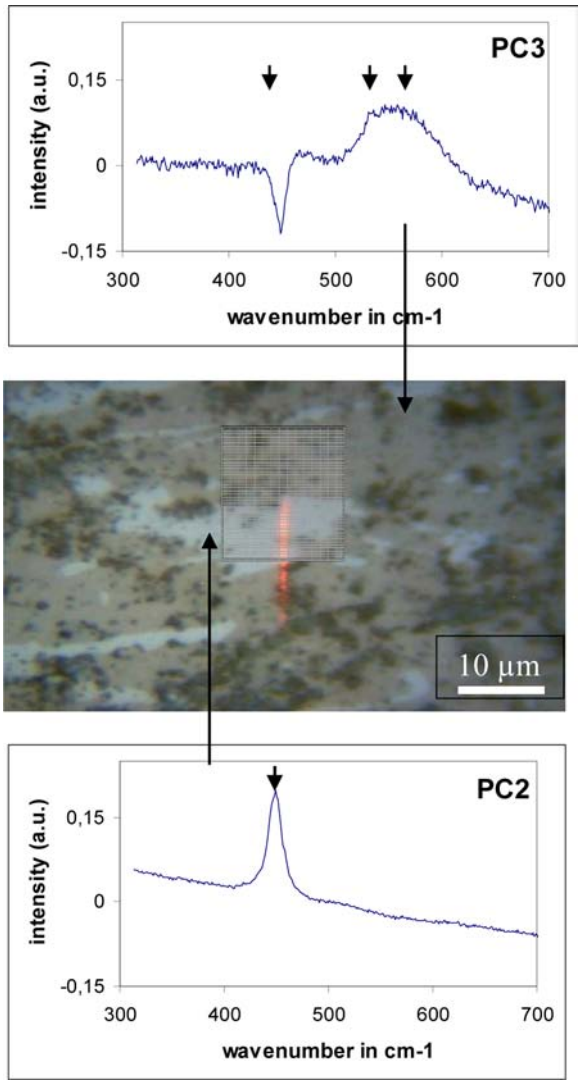

Figure 1. Optical microscopy on a cross section of the $(U_{.923},Nd_{.077})O_2$ sample. The 16 × 66 points, 16 × 16 μm^2 mapping of Raman measured points is represented by a grid in white. PC2 and PC3 deduced from PCA corresponding to the white and gray areas, respectively, of this cross section re below and above optical image, respectively; the arrows indicate identified peaks.

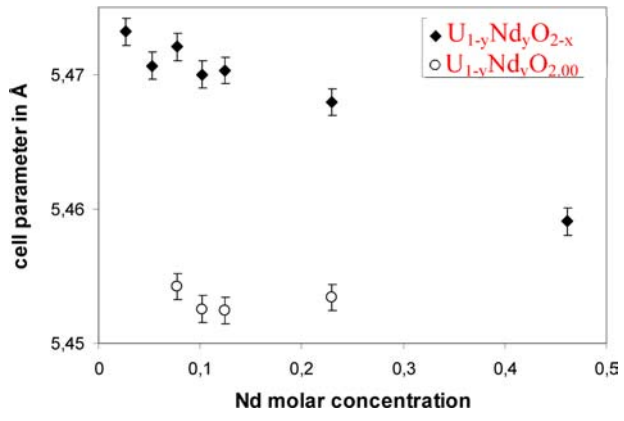

Figure 2. Unit cell parameter of the two phases as a function of the calculated Nd content in moles.

our case with $(U,Nd)O_{2\pm x}$ samples because the two phases we observed were also fabricated separately in thermodynamic equilibrium conditions for the same Nd content but different oxygen stoichiometry in ref 13 and cannot be considered as mixed metastable phases. In our case, because we simultaneously observed two phases on the $(U,Nd)O_{2\pm x}$ samples,[7] a biphasic domain has to be considered.

We attribute this biphasic domain to a miscibility gap in the U−Nd−O phase diagram (Figure 3) consistently with other

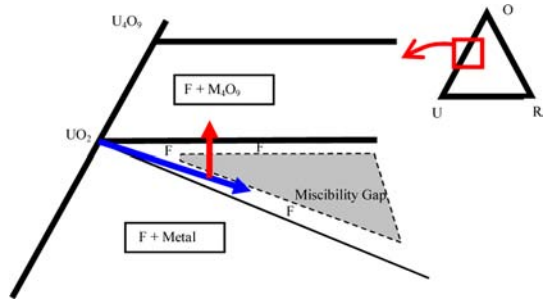

Figure 3. Miscibility gap in the U−R−O phase diagram. F is a UO_2-derived fluorite phase. The blue line is a tentative representation of the irradiated UO_2 chemical state, whose content in rare earth increases with burnup. The red line is a tentative representation of the chemical state of spent fuel submitted to oxidation when in contact with the atmosphere (see the text for details).

already reported miscibility gaps in the oxygen under stoichiometric parts of the U−Pu−O[14] and U−Ce−O[15] phase diagrams. Following Ohmichi et al. analysis, we interpret the formation of this miscibility gap as a competition between oxygen vacancy and U^{5+} cation formation in order to ensure electroneutrality in $(U,Nd)O_{2\pm x}$. Ohmichi et al. considered indeed that, in a $U_{1-y}R_yO_{2.00}$-type solid solution, U^{5+} cations are created in order to compensate for Nd^{3+} incorporation in UO_2, while in $U_{1-y}R_yO_{2-x}$ oxygen vacancies are created for that purpose.

The Raman results can be interpreted consistently with this assumption. The cell parameter of the gray phase has a linear dependence on the Nd content that corresponds to the behavior of $U_{1-y}R_yO_{2-x}$ in ref 10. The incorporation of oxygen vacancy in the UO_2 lattice induces a lower local symmetry and changes in the bonding of the surrounding atoms. Thus, in the Raman spectrum of the $(U,Nd)O_{2-x}$ gray phase, the peak at 570 cm^{-1} could be interpreted as a UO_2 Raman-forbidden mode that becomes active because of lower symmetry and the peak at 530 cm^{-1} could be interpreted as a local phonon mode associated with oxygen-vacancy-induced lattice distortion. This last attribution is consistent with the interpretation of additional vibrational modes observed in Ce^{IV}−R−O systems at wavenumbers higher than the Raman-active mode in CeO_2, which are also attributed to oxygen vacancies.[16,17] On the contrary, no modification of UO_2 Raman spectra is observed on the white phase because it would correspond to $U_{1-y}R_yO_{2.00}$ in which Nd^{3+}−U^{5+} cations induce no local symmetry changes in the UO_2 lattice.

It is very likely that the miscibility gap we consider in the U−Nd−O phase diagram also exists in other U−R−O phase diagrams. For example, the coexistence of two phases with different cell parameters observed on $Eu_yU_{1-y}O_{2\pm x}$ samples[18] could be reinterpreted with this hypothesis. The limits of the miscibility gap in U−R−O phase diagrams should be

dx.doi.org/10.1021/ic301100c | Inorg. Chem. 2012, 51, 9147−9149

determined because the behavior of irradiated UO_2 could be described more precisely with this information.

During its irradiation in a nuclear reactor in a reducing environment, UO_2 is indeed progressively doped with fission products (FPs), more specifically with rare earths, so that it can be considered as a $(U,FP)O_{2-x}$ compound because it remains stoichiometric or slightly hypostoichiometric up to burnup in the range of 70−80 GWd/tU.[19] Knowing all the U−R−O phase diagrams, where R is also FP, the chemical state of irradiated UO_2 could be described by its position on an equivalent U−FP−O phase diagram, with this position moving during irradiation (blue line in Figure 3). This line could cross a possible miscibility gap because the molar content of plutonium and rare-earth FPs reaches 5% for burnup in the range of 70−80 GWd/tU and because the miscibility was observed in the U−Nd−O system above 5% Nd molar concentration.

A possible accidental scenario that might be studied in the frame of the Fukushima accident would consist of the dispersion of irradiated fuel at a temperature of around 100 °C from a defective fuel element located in storage pool in air. Air oxidation of irradiated UO_2 can lead to chemical transformation before the formation of a M_4O_9 phase (M stands for U + FP) that is observed upon air oxidation[20] by thermogravimetric analysis. The oxidation of $(U,FP)O_{2-x}$ could also result in the crossing of the miscibility gap (red line in Figure 3) and hence a significant change of its properties. The chemical state of irradiated UO_2 dispersed in the environment at low temperature would depend on its position on the equivalent U−FP−O phase diagram as a function of the oxygen quantity adsorbed by the pristine irradiated UO_2 during high-temperature exposure.

In all cases, taking into the existence of a miscibility gap in the U−R−O phase diagram will provide a more accurate description of irradiated uranium oxide and could be a fruitful area of research in order to reduce the impact of uranium oxide in the environment.

■ ASSOCIATED CONTENT

Supporting Information

Experimental details and Raman spectra. This material is available free of charge via the Internet at http://pubs.acs.org.

■ AUTHOR INFORMATION

Corresponding Author

*E-mail: lionel.desgranges@cea.fr.

Notes

The authors declare no competing financial interest.

■ ACKNOWLEDGMENTS

The authors thank L. Sylvestre for sample preparation. The authors are indebted to the program PERCOX, funded by CEA, and also to MATINEX GNR.

■ REFERENCES

(1) http://www.nature.com/news/specials/japanquake/index.html.
(2) Final Report EUR 16857: Oklo natural analogue, Office for Official Publications of the European Communities, 1996.
(3) Gauthier-Lafaye, F. *Nature* **1997**, *387*, 337−337.
(4) Diehl, H. G.; Keller, C. *J. Solid State Chem.* **1971**, *3*, 621−636.
(5) Keller, C.; Boroujjerdi, A. *Inorg. Nucl. Chem.* **1972**, *34*, 1187−1193.
(6) Lindemer, T. B.; Brynestad, J. *Am. Ceram. Soc.* **1986**, *69*, 867−876.
(7) Desgranges, L.; Marcet, M.; Pontillon, Y.; Porcher, F.; Lamontagne, J.; Matheron, P.; Iltis, X.; Baldinozzi, G. *Solid State Phenom.* **2011**, *172−174*, 624−629.
(8) Graves, P. R. *Appl. Spectrosc.* **1990**, *44*, 1665−1667.
(9) Livneh, T; Sterer, E. *Phys. Rev. B* **2006**, *73*, 085118.
(10) Desgranges, L.; Baldinozzi, G.; Rousseau, G.; Niépce, J. C.; Calvarin, G. *Inorg. Chem.* **2009**, *48*, 7585−7592.
(11) Ohmichi, T.; Fukushima, S.; Maeda, A.; Watanabe, H. *J. Nucl. Mater.* **1996**, *102*, 40−46.
(12) Fujino, T.; Ouchi, K.; Mozumi, Y.; Ueda, R.; Tagawa, H. *J. Mater. Nucl.* **1990**, *174*, 92−101.
(13) Hinatu, Y.; Fujino, T. *J. Solid State Chem.* **1988**, *73*, 388−397.
(14) Gardner, E. R.; Markin, T. L.; Street, R. *J. Inorg. Nucl. Chem.* **1965**, *27*, 541−551.
(15) Martin, T. L.; Street, S.; Crouch, E. C.. *J. Inorg. Nucl. Chem.* **1970**, *32*, 59.
(16) Horlait, D.; et al. *Chem.* **2011**, *50*, 7150.
(17) McBride, J. R.; Hass, K. C.; Poindexer, B. D.; Weber, W. H. *J. Appl. Phys.* **1994**, *76*, 2435.
(18) Fujino, T.; Ouchi, K.; Mozumi, Y.; Ueda, R.; Tagawa, H. *J. Mater. Nucl.* **1990**, *174*, 92−101.
(19) Spino, J.; Peerani, P. *J. Nucl. Mater.* **2008**, *375*, 8−25.
(20) Kim, J.; Ha, Y.; Park, S.; Jee, K.; Kim, W. *J. Nucl. Mater.* **2001**, *297*, 327−331.